

---

# Trajectory following method for on-line reconfiguration and recovery after actuator jamming

Dominique Tristrant

[Dominique.Tristrant@onera.fr](mailto:Dominique.Tristrant@onera.fr)

+33 490170135

ONERA - Centre of Salon de Provence

Base Aérienne 701 - Ecole de l'Air

13661 Salon Air – France

## ABSTRACT

A trajectory following methodology is presented in this paper with applications to rotorcraft flight dynamics, in particular to control and recover aircraft after a swashplate actuator jamming. This type of failure which is very severe with regards to aircraft controllability and flight safety has been studied to test and evaluate the capabilities and performance of the methodology. Actuator jamming is considered as catastrophic because it often results in a complete loss of control of aircraft. To recover aircraft and manage such a failure two complementary tasks have been here considered: the control method and the guidance strategy.

A nonlinear model predictive control method that has been developed for controlling aircraft is first presented. It consists in following a reference trajectory calculated online by the guidance strategy. Stability and robustness of this predictive control method are analysed in a linear approach in order to tune the main control parameters in every flight phase of the desired trajectory. This method does not require any assumption on its flight dynamics model which is nonlinear and comprises various cross couplings as well as different aerodynamic interferences between aircraft elements. The trajectory following method has been demonstrated to be efficient for performing automatic flight from the definition of a set of waypoints.

Secondly, the guidance strategy that has been developed to proceed to an emergency landing procedure in the best conditions is presented. The trajectory is chosen to optimise the capabilities of controlling the aircraft behaviour. The strategy consists of maintaining the aircraft as close as possible to its equilibrium conditions while taking into account the actuator jamming and its consequences on aircraft controllability. Thus, the proposed guidance strategy defines a way to proceed to an emergency landing in minimising the hazards and the risks of loss of control resulting from the failure.

Simulations are performed to evaluate methodology performances and to demonstrate its stability and robustness capabilities. To test and evaluate the methodology simulations have been conducted in different cases: with jamming of different swashplate actuators; in conducting two types of emergency landing procedures: a run-on landing or a normal landing with a quasi-vertical touchdown; and also in considering different initial conditions of aircraft flight parameters when the failure occurs.

These demonstrations have been performed in simulations of a generic helicopter with a nonlinear model taking into account mechanical constraints inherent to helicopters such as limitations in rotor speed and in engine torque.

## 1. ABBREVIATIONS and ACRONYMES

$\mathcal{R}_0$	: earth reference axis system	$L_{ON}$	: longitudinal cyclic position ( $-1 < L_{ON} < 1$ )
$\mathcal{R}$	: aircraft reference axis system	$L_{AT}$	: lateral cyclic position ( $-1 < L_{AT} < 1$ )
theta or $\theta$	: aircraft pitch attitude (Euler angle)	$P_{ed}$	: pedals position ( $-1 < P_{ed} < 1$ )
phi or $\phi$	: aircraft roll attitude (Euler angle)	$\chi$ or $khi$	: track angle
psi or $\psi$	: aircraft heading (Euler angle)	$\lambda_1, \lambda_2, \text{ and } \lambda_3$	: positions of the 3actuators (jacks)
$X_g, Y_g, Z_g$	: coordinates of the aircraft centre of mass in $\mathcal{R}_0$	$\theta_0, \theta_{1c} \text{ and } \theta_{1s}$	: pitch angles of the rotor blades
$V_N, V_E$	: North and East ground velocities	ref	: index relative to the reference trajectory
$V_H$	: aerodynamic speed component in the horizontal plane	R	: swash plate radius
$C_{OL}$	: collective stick position ( $0 < C_{OL} < 1$ )	E	: eccentricity of the blade rods

---

---

$U, V_{lat}$	: longitudinal, lateral components in $\mathcal{R}_0$ of the aerodynamic velocity	$h$	: time horizon = $p \cdot \Delta t$
$V_z$	: vertical velocity in $\mathcal{R}_0$ (positive in climb)	<b>A, B, C</b>	: state, input and output <b>matrices</b> of the linearized continuous system
$W_N, W_E, W_Z$	: North, East and vertical wind components in $\mathcal{R}_0$	$X_k$	: aircraft state vector at instant $t = k \cdot \Delta t$
$p, q,$ and $r$	: angular velocities in roll, pitch and yaw	$Y_k$	: aircraft output vector
<b>J</b>	: criterion of distance between calculated and desired trajectories	$\hat{X}_k$	: model state vector at $t = k \cdot \Delta t$
<b>H</b>	: height with respect to the ground	$\hat{X}_k^{k+1 k}$	: predicted state vector at $(k+1)\Delta t$
$C_{equ}$	: equilibrium criterion	$\delta_k$	: control vector (system input)
<b>IGE</b>	: In Ground Effect	<b>R<sub>k</sub></b>	: reference vector (target to reach)
<b>OGE</b>	: Out of Ground Effect	<b>W<sub>k</sub></b>	: wind disturbance vector (expressed in the $X_k$ axis system)
$\Delta t$	: step in time	$\vartheta_k$	: state noise vector
		$\mathcal{D}$	: domain of accessible controls

## 2. INTRODUCTION

As a failure of a control effector or a critical surface occurs in flight, quick actions must be undertaken to keep aircraft control and assure the safety of flight. Reconfiguration of the flight control aims at accommodating a failure to adapt the control system and mitigate effects of failure. For fixed-wing aircraft, flight control reconfiguration has been well proven through the development of various methods in taking advantage of existing control surfaces or effector redundancies. If existing redundancies could be a solution in some cases, in contrast with fixed-wing there is no redundant control surface on a helicopter. Moreover, the redundancy of conventional actuators cannot solve the problem of a swashplate actuator jamming or freezing. This type of failure is very severe with regards to aircraft controllability and flight safety. It is considered as catastrophic, resulting often in a complete loss of control of aircraft.

Underlying the need to find out a solution to this safety problem the Clean Sky Joint Technology Initiative published a call for developing an adequate technology<sup>[1]</sup>. The goal is to conceive a disconnect device for jam-tolerant linear actuators, in particular for swashplate actuation. In this challenge, any jammed actuator could be disconnected without preventing the redundant one of being still effective. The European project FASTDISC<sup>[2]</sup> aims at developing an innovative technology which could be a hardware solution to swashplate actuator jamming.

Another type of solution, comprising hardware and software aspects, has been proposed by R. Enns and J. Si<sup>[3]</sup>. However, in this approach the swashplate geometry and actuator positions must be first redesigned in order to optimise actuator configuration on the swashplate so that the control cross couplings are maximised while actuator range of displacement is kept not too large. In addition, this method assumes that the actuator can be designed to lock into a predetermined position. When the failure occurs the reconfiguration of the control system permits to maintain the control of pitch and roll attitudes but it sacrifices the control of the vertical axis whereas some strategies are proposed to compensate for the lost vertical control.

As a matter of fact, only very few methods have been studied to really handle the general case of a swashplate actuator jamming on existing or conventional helicopter. To treat and manage completely such a failure up to

aircraft landing no method or control strategy has been identified in the bibliography.

This paper is proposing a methodology aiming at managing the complete flight phase from failure recognition up to the helicopter emergency landing.

This methodology contains at the same time a trajectory following method for controlling aircraft and a guidance strategy adapted to the loss of controllability resulting from actuator jamming.

The trajectory following method is presented in chapter 3. It is based on the Model Predictive Control method, initially developed by J. Richalet et al.<sup>[4]</sup> for controlling complex processes, particularly in the chemical industry. Later this method was generalised by D.W Clarke<sup>[5]</sup>. Many papers have then been published in this field with various developments and applications. S.J Qin and T.A. Badgwell provide a survey of industrial model predictive control technology<sup>[6]</sup>. For controlling systems and robots F. Allgöwer et al.<sup>[7]</sup> describe of the Nonlinear Model Predictive Control method with its properties. An interesting and practical approach is also developed by J.A Rossiter<sup>[8]</sup>.

The chapter 3 presents the specificities of the nonlinear model predictive control method which has been developed in this paper to control and recover aircraft after actuator failure occurrence. Basically, this method consists in following a reference trajectory in taking advantage of aircraft behaviour predictions performed on a given horizon of time by means of a flight dynamics model as realistic as possible. Then, to illustrate the control method capabilities, its application to automatic flight is presented.

In chapter 4 is then presented the rotor swashplate kinematics and the consequences of one actuator jamming on rotor control capabilities.

To assure the safety of flight and proceed to an emergency landing the tracked trajectory must be defined by taking into account the reduced aircraft controllability. This is the purpose of the guidance strategy presented in chapter 5.

The main objective of this work was to assess the potential capabilities of the methodology to manage failure situations. This assessment has been conducted in chapter 6 where are presented various simulation results

---

in different cases of actuator jamming and different flight situations.

All these assessments have been conducted by the use of a generic but realistic nonlinear model of a twin turbine helicopter of medium mass.

### 3. FOLLOWING TRAJECTORY METHOD

#### 3.1. Description of the method

The objective is first to determine, at each current time  $t$ , the 'optimal' control input  $\delta^*(t)$  for which the reference and predicted trajectories match as much as possible. A flight dynamics model is necessary to predict at the current time  $t$ , the helicopter flight trajectory over a certain predefined horizon of time  $h$ .

The reference trajectory is supposed to be known from on-line calculations provided by the guidance law. For controlling aircraft on-line, it is preferable that the reference trajectory is redefined at every step in time by taking into account actual flight conditions.

In this method, at time  $t$  the aircraft trajectory is predicted over the time horizon  $h$  with a control input  $\delta(t)$  set at a constant value. The unknown input vector  $\delta(t)$  is calculated in an iterative process to make the predicted flight variables as close as possible to the desired reference target in minimising a quadratic criterion  $J$  expressing the gap between the two trajectories.

Thus, at each iterative step numbered  $k$ , the control input vector  $\delta$  minimizes the criterion  $J$  defined as:

$$(1) J^2 = \frac{1}{2} \cdot \sum_{i=1}^N \pi_i \cdot [F_i(\delta(t), t+h) - R_i(t+h)]^2$$

where  $R(t+h)$  denotes the reference vector of dimension  $N$  which is targeted at time  $t$ ,  $F_i(\delta(t), t+h)$  denotes the flight parameter vector predicted at the time horizon  $t+h$  as a function of the control input vector  $\delta(t)$ , and  $\pi$  denotes the weighting vector of the tracked flight parameters.

The minimization algorithm is based on a gradient method that is different from the classical Newton's method. Indeed, depending on flight conditions the Jacobian matrix of the system could be poorly conditioned or locally degenerated (e.g.: due to a loss of control effectiveness or a control saturation), and would be therefore inappropriate to an inversion process. Moreover, resulting of the non-linear nature of the model, the calculations of second derivatives and matrix inversions could induce serious numerical problems. So, the optimisation method in use is limited to first order derivations of the model and does not require any matrix inversion.

The 'optimal' input  $\delta^*(t)$  calculated in adjusting the predicted trajectory close to the reference target on the time horizon  $[t, t+h]$ , is then applied to the system to obtain the aircraft flight parameters at the next incremental time,  $t_1 = t + \Delta t$ . At this new time,  $t_1$ , the process is repeated to calculate new predictions with a new input vector on the same time horizon length, i.e.  $[t_1, t_1+h]$ . Thus, the 'optimal' input  $\delta^*(t)$  has been applied only until the next time step where the control inputs are re-evaluated in using the aircraft state data at time  $t_1$ . The terminology 'receding horizon' is often used to express

that the horizon is constantly moving away, at the same speed at which the aircraft is moving.

The main advantages of this method are:

- A complete and realistic nonlinear flight dynamics model of the aircraft can be used to control flight, without requiring any additional linearization or assumption;
- To define control inputs the method does not only consider data at current time but takes also into account some data in the future calculated on a given horizon of time;
- Constraints on control inputs and controlled flight parameters are directly taken into account in the method to predict flight path and to calculate inputs;
- No matrix inversion is required in the process;
- Processing can be carried out on line.

In the conventional predictive control method several control input vectors are simultaneously calculated on the time horizon to match reference and prediction:

$\delta(t+j\Delta t)$  with  $j = 0, 1, \dots, l$  and  $(t+j\Delta t) \in [t, t+h]$ .

However in that case calculations are heavier and require also matrix inversion to solve the set of control input vectors.

It is recognised that predictive control belongs to the class of the optimal control laws; however in practice the control method is here suboptimal. Indeed, the control vector calculated at each step in time is unique. Calculations are then simpler and fast enough to proceed online. Moreover, as shown hereafter, the closed loop control of the linearized system can then be analytically expressed so that its stability and performance with respect to control parameters can be more easily studied.

#### 3.2 Stability and performances

The stability and performance of the predictive control method in use have been studied in assuming that the aircraft flight dynamics equations can be locally linearized. These equations are here expressed as follows:

$$\frac{d\mathbf{X}(t)}{dt} = \mathbf{A}(\mathbf{X}(t)+\mathbf{W}(t))+\mathbf{B}\delta(t) \text{ aircraft state equation}$$

$$\mathbf{Y}(t) = \mathbf{C}\mathbf{X}(t) \text{ output equation}$$

$$\hat{\mathbf{X}}(t) = \mathbf{X}(t)+\mathbf{\vartheta}(t) \text{ state estimate equation}$$

In these equations,  $\mathbf{W}(t)$  denotes the disturbance vector (e.g. the wind) exerted on the aircraft, and  $\mathbf{\vartheta}(t)$  is the measurement noise vector on the state vector estimate. To study stability it is assumed that the model equations have been previously calibrated in flight so that they match well to the system equations; the noise of modelling has then been neglected in a first approach. However in chapter 5 the effect of discrepancies between model and system will be tested in simulations with the nonlinear predictive method.

As numerical computing requires sampling of data, the analyses have to conduct with discrete formulations of dynamic equations. These discrete formulations of the system equations can be expressed with the following state-space models:

$$\mathbf{X}_{k+1} = \mathbf{E}(\mathbf{X}_k + \mathbf{W}_k) + \Delta t \cdot \mathbf{B} \delta_k + \mathbf{\vartheta}_k ; \mathbf{Y}_k = \mathbf{C} \mathbf{X}_k$$

where  $\mathbf{E} = \mathbf{I} + \Delta t \cdot \mathbf{A}$

$\mathbf{X}_k$  and  $\mathbf{Y}_k$  are respectively the values of the state and output vectors at the current time  $t$  which corresponds to the  $k$ -th sampling instant from the initial time.

As shown in appendix 1, the control vector is calculated to minimise  $\mathbf{J}_k$  the squared distance between the output vector  $\hat{\mathbf{Y}}_{k+p|k}$  predicted at  $p$  time steps ( $h=p\Delta t$ ) further to

the current time  $t$ , and the desired reference vector  $\mathbf{R}_{k+p}$  :

$$(\rho) \mathbf{J}_k = \frac{1}{2} (\hat{\mathbf{Y}}_{k+p|k} - \mathbf{R}_{k+p})^T \mathbf{P} (\hat{\mathbf{Y}}_{k+p|k} - \mathbf{R}_{k+p}) \quad \text{where}$$

$\mathbf{P}$  denotes a semi positive diagonal weighting matrix.

When  $\delta_k$  is kept constant on the prediction horizon, the control equation in closed loop can then be expressed as follows:

$$\beta) \mathbf{X}_{k+1} = \mathbf{S}\mathbf{X}_k + \mathbf{T}\mathbf{R}_{k+p} + \mathbf{E}\mathbf{W}_k + \mathbf{N}\mathbf{v}_k + \mathbf{K}\mathbf{d}\mathbf{J}_{\min}$$

$$\text{where } \mathbf{K} = \Delta t \cdot \mathbf{B}^{-1} \mathbf{H}^T \mathbf{C}^T \mathbf{P} \mathbf{C} \mathbf{H} \mathbf{J}^{-1}$$

$$\mathbf{H} = \Delta t \cdot (\mathbf{E}^p - \mathbf{I}) \mathbf{E}^{-1} \mathbf{J}^{-1} \mathbf{B}$$

$$\mathbf{T} = \Delta t \cdot \mathbf{B}^{-1} \mathbf{H}^T \mathbf{C}^T \mathbf{P} \mathbf{C} \mathbf{H} \mathbf{J}^{-1} \mathbf{H}^T \mathbf{C}^T \mathbf{P}$$

$$\mathbf{N} = \mathbf{T} \mathbf{C} \mathbf{E}^p \quad \text{and} \quad \mathbf{S} = (\mathbf{E} - \mathbf{T} \mathbf{C} \mathbf{E}^p)$$

In this expression  $\mathbf{d}\mathbf{J}_{\min}$  is the value of the criterion gradient  $\mathbf{d}\mathbf{J}$  as  $\mathbf{J}$  is minimal. When  $\mathbf{d}\mathbf{J}_{\min}$  can be set to zero there is no deficiency to reach the reference vector at the time horizon. However it must be considered that it is not always possible to make  $\mathbf{d}\mathbf{J}_{\min}$  equal to zero by means of controls, particularly when at least one component of the control vector is jammed or saturated.

The transfer matrix  $\mathbf{K} = \Delta t \cdot \mathbf{B}^{-1} \mathbf{H}^T \mathbf{C}^T \mathbf{P} \mathbf{C} \mathbf{H} \mathbf{J}^{-1}$  between the system state vector and  $\mathbf{d}\mathbf{J}_{\min}$  expresses the impact on the state vector of the control deficiency to make identical the output vector  $\mathbf{Y}$  and the targeted reference vector  $\mathbf{R}$ .

The matrices  $\mathbf{S}$ ,  $\mathbf{N}$ ,  $\mathbf{T}$  and  $\mathbf{K}$  are dependent upon the control parameters  $p$  and  $\mathbf{P}$ , defining respectively the prediction horizon length and the diagonal matrix weighting the components of the discrepancy between the predicted output vector and the desired reference vector. As will be illustrated later, this linear approach will be used to tune the parameters of the model predictive control loop for adapting stability and performance in each flight phase of the reference trajectory.

### 3.3 Model characteristics:

Simulations are conducted with a nonlinear model of a generic helicopter of the Dolphin class (twin turbine helicopter, mass= 3.5tons, rotor articulated). It comprises various cross couplings as well as different aerodynamic interferences between aircraft elements.

The aircraft limitations considered in this paper are:

- Power max of engine: 526Kw (at take-off),
- rotor rate between 91% and 113%,
- max torque of 107%.

The actuator model comprises:

- lower and upper stops,
- dynamics behaviour of a first order transfer function with a time constant set to 0.5s,
- saturation in displacement speed at 150mm/s.

### 3.4 Application to automatic flight:

An applicative example of the following trajectory method demonstrates the automatic control of an helicopter whose

flight plan is defined by a set of waypoints as shown in the Table 1 hereafter.

$X_g$ -North (m)	$Y_g$ -East (m)	$Z_g$ (m)	$U$ (m/s)
1000.	200	1000	40
1800	250	1020	50
1800	-100	1000	20
2750	-200	1030	10

The flight plan is here constituted of a set of 4 waypoints, each one is described by three geographic coordinates ( $X_g$ ,  $Y_g$ ,  $Z_g$ ) and the longitudinal velocity to

fly. At its initial conditions ( $X_g=0$ ,  $Y_g=0$ ,  $Z_g=1000\text{m}$ ) the helicopter flight is assumed to be stabilised at 40m/s at level.

A reference trajectory joining the different waypoints is calculated with account of constraints relative to aircraft performances in vertical and longitudinal accelerations and with a rate of turn limited in dynamics to a first order function and a time constant set to 0.5s.

The predictive control method is then conducted in simulation as defined previously to track the aircraft positions ( $X_g, Y_g, Z_g$ ) as functions of time (4D trajectory) in performing a flight with a lateral velocity equal to zero (no sideslip). In Figure 1 are presented the simulation results of the nonlinear model with a prediction horizon set to 2s for all flight phases. To simulate noise measurements a Gaussian white noise has been added in the estimate of the state vector that is used to calculate inputs of the control law. The four plots presented are respectively: the flight path and the waypoints in the horizontal plane (1.a), the longitudinal and lateral velocities (1.b), the longitudinal and lateral attitudes (1.c) and the controls activities (1.d).

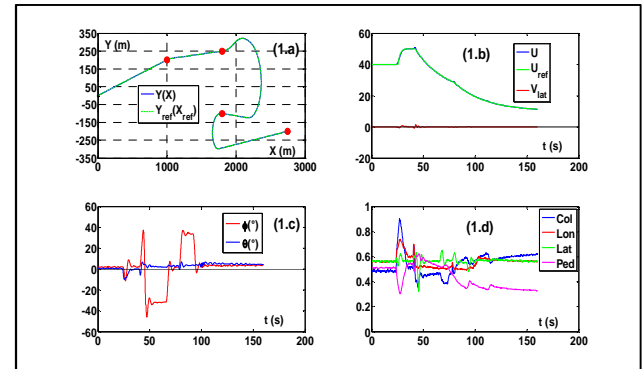


Figure 1: Automatic flight achieved from a flight plan

In this case  $h=2\text{s}$  and the flight plan is well followed as required (Figure 1).

Figure 2 shows the effect of the prediction horizon on 3 main control law characteristics which are referring to equation (3). In this equation:

-  $\mathbf{S}$  denotes the state vector matrix of the discrete system in closed-loop. As shown in Appendix 1, in the continuous form of the control equation the eigen values positions in the complex plane of the  $\mathbf{F}$ -matrix will characterise the stability of the system (fig.1.a),

-  $\mathbf{N} = \mathbf{T} \mathbf{C} \mathbf{E}^p$  is the transfer matrix between the noise and state vectors. Its norm characterises the sensitivity of the control loop to the state noise vector  $\mathbf{v}$  (fig. 2.b),

-  $\mathbf{T}$  denotes the transfer matrix between the tracked reference vector and the system state vector. Its norm will characterise the gain to reach the reference  $\mathbf{R}$  by means of controls (fig. 2.c).

It can be noted that the system is unstable in open loop (fig. 2.a) and a prediction time horizon equal to 2s permits

not only to guarantee a good level of stability but also a low noise sensitivity while the gain required to track the reference is not too large in order to avoid any saturation of flight controls.

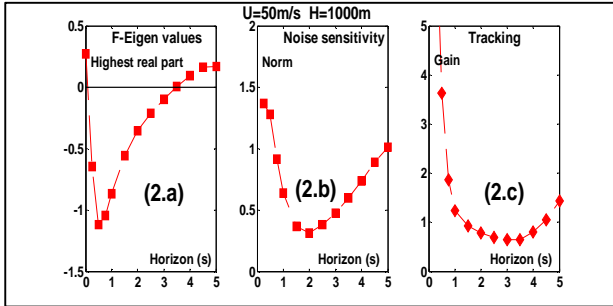


Figure 2: Effect of the prediction horizon on control law characteristics

Now, in Figure 3 simulation results are compared for three values of the predictive time horizon, respectively 1.5s, 2s and 4s. In these three cases, the plots from left to right present the simulated and reference altitudes, the collective activity, and the resulting lateral attitude of aircraft. The tendencies on the control law characteristics predicted by the linear approach are confirmed. Indeed, stability in altitude is less good with  $h=4s$  (fig 3.a). For  $h=1.5s$  the trajectory is more sensitive to state noise (fig 3.c) and the collective demand required for tracking reference is higher (fig 3.b).

The choice of predictive time horizon set to 2s is a good compromise and provides satisfactory results to follow the reference trajectory (Figure 1).

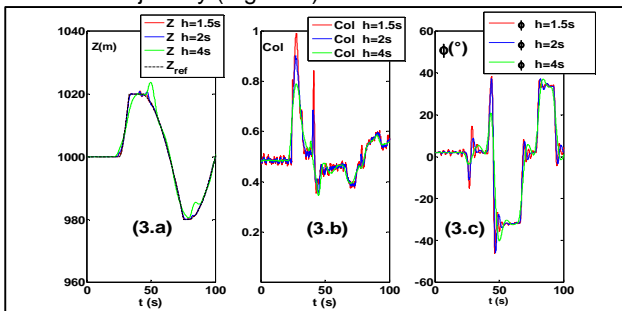


Figure 3: Comparison of simulation results for different predictive time horizons (1.5s, 2s and 4s)

#### 4. ROTOR KINEMATICS and JAMMING

The main application studied in this paper concerns the failure of one main rotor swashplate.

In a previous work<sup>[9]</sup> a kinematics model of a generic swashplate was developed and integrated into the simulation code of the generic helicopter that is equipped with a fully articulated rotor. Figure 4 below illustrates the general principles of the swashplate kinematics. The swashplate positioning is achieved by means of 3 independent actuators:  $\lambda_1$  located in the longitudinal plane of aircraft,  $\lambda_2$  and  $\lambda_3$  which are diametrically opposite in the lateral plane.

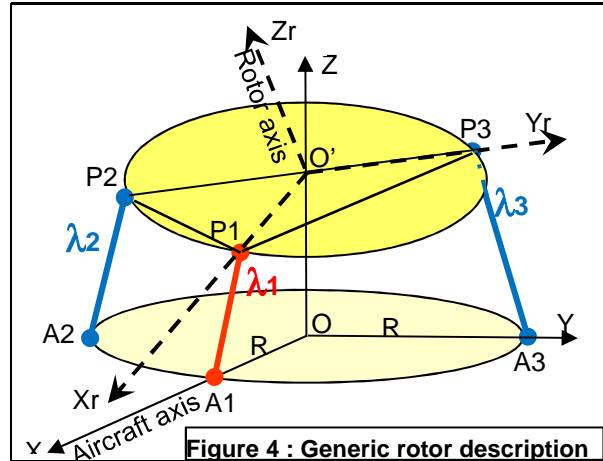


Figure 4: Generic rotor description

These 3 actuators provide 3 degrees of freedom to position the circular swashplate whose displacement can thus be controlled in height (collective effect) and in angular orientation according to two distinct angles (longitudinal and lateral cyclic effects). The control of the 3 swashplate degrees of freedom is obtained by the elongation of the 3 actuators ( $\lambda_i$ ), in order to control the blade pitch angles:  $\theta_0$ ,  $\theta_{1c}$  and  $\theta_{1s}$ , via the rotor blade rods. The kinematics equations relating actuator elongations of a generic swashplate and blade pitch angles are described in appendix 2.

If one of these actuators is blocked at a fixed position, then only 2 actuators are operational and one dimension of degree of freedom is lost to position the swashplate and the blade pitch angles, reducing thus the capabilities to control the main rotor and the helicopter motion. As mentioned in appendix 2 two blade pitch angles are then linked by a quasi linear relationship. This type of failure is very severe. In the absence of any redundant control surface, the manoeuvring capabilities of the helicopter are drastically reduced and the pilot can quickly lose the control of aircraft.

In addition to the loss of one degree of freedom to control aircraft, the pilot encounters another problem in flight because this type of failure is also difficult to manage from an ergonomic point of view. Indeed, helicopters have generally a system called 'mixer' which relates, via the swashplate actuator displacements, the pilot's commands to blade angles so that the control of blade angles is decoupled. The collective and the cyclic blade pitch angles can then be controlled directly in response to pilot commands on vertical, longitudinal and lateral axes. However, in the case of an actuator jamming the existing mixer logic is no more appropriate to control blade pitch angles and the effects of pilot actions on the sticks becomes unusual and may be upsetting.

To illustrate the effects of actuator jamming on aircraft controllability the figure 5 compares the domains of rotor pitch angles accessible with all actuators available (grey area) with the case resulting of the actuator 2 jamming (blue area) at a value corresponding to a stabilised flight at 40m/s.

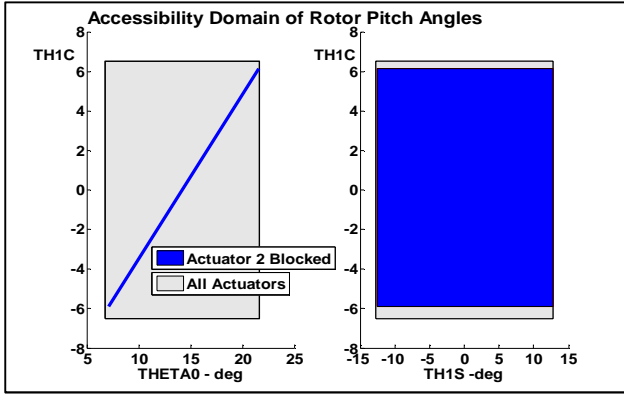


**Figure 5 : Effect of actuator 2 jamming on pitch angles accessibility**

When actuator 2 is blocked the  $\theta_0$  and  $\theta_{1c}$  pitch angles are then linked in a linear dependence. Here it results also a slight reduction in the range of the possible  $\theta_{1c}$  excursion.

## 5. GUIDANCE STRATEGY

Now we consider the situation when an actuator jamming is detected and identified while the helicopter is in stabilised flight.

As seen previously, one actuator jamming leads to a significant reduction of the aircraft controllability. The loss of aircraft controllability will reduce its manoeuvrability and will limit its capabilities to balance the flight and to counter external disturbances or wind gusts encountered in flight. In order to land the aircraft in the best possible conditions in an emergency procedure, the guidance trajectory must be designed with account of the lack of controllability and 'stabilizability' of the aircraft. This design has to be achieved in the appropriate part of the flight domain.

### 5.1 Equilibrium criteria

The objective of the proposed guidance and landing procedure is to define a reference trajectory where the aircraft will be as close as possible to accessible equilibrium conditions, with the account of its actual control capabilities.

Defining the equilibrium conditions of aircraft at given velocity and altitude consists in calculating the values of the 4 control inputs ( $C_{OL}$ ,  $L_{ON}$ ,  $L_{AT}$ ) and 2 attitude angles ( $\theta$  and  $\phi$ ) which make the 6 linear and angular accelerations equal to zero. Here will be considered as control inputs the 3 swashplate actuators ( $\lambda_i$ ), which permit to modify the rotor thrust in magnitude and orientation via the blade pitch angles, and the pedals ( $P_{ed}$ ) which control the rear rotor thrust via its own blade pitch angle. In the flight domain, the aircraft equilibrium (or trim) conditions are determined by solving a system of 6 equations (accelerations) by means of 6 parameters (control inputs and attitudes). When one control input is blocked to a constant position it is not possible to solve the system at each point of the flight domain. The trim conditions can then exist only in a subset of the flight domain.

The equilibrium criterion is defined as follows:

$$C_{equ}(H, U, V_{lat}, V_z) = \min_{\delta_j \notin D} \left( \dot{p}^2 + \dot{q}^2 + \dot{r}^2 + \dot{U}^2 + \dot{V}_{lat}^2 + \dot{V}_z^2 \right)$$

Knowing the elongation of the jammed actuator; at each point of the flight domain the equilibrium criterion  $C_{equ}$  can be calculated. In the flight domain, this criterion depends mainly on the three velocity components. The altitude and aircraft mass are also influent but at a much lower extent.

At an equilibrium point this criterion is null. When  $C_{equ}$  is not null, its value characterises the global residue in linear and angular acceleration which cannot be cancelled by means of controls. Consequently, the more the magnitude of this equilibrium criterion (or residual acceleration) will be large, the more it will be difficult to stabilise the flight and to follow a given trajectory.

### 5.2 Reference trajectory definition

The mapping of  $C_{equ}$  in the flight domain will permit to design a guidance trajectory which minimises the residual acceleration for flying from a given point to another point in the flight domain. In analysing this mapping some flight points for which  $C_{equ}$  is fairly small can be selected to constitute the 'waypoints' of the desired reference trajectory.

This criterion can be pre-calculated in the whole flight domain and stored in an onboard data basis. When the actuator failure is detected in flight, the subset corresponding to the value of the jammed actuator can be extracted from the data basis to choose adequate waypoints and define online a suitable guidance trajectory.

The best set of waypoints can then be defined to reach a chosen landing condition while following a route where the equilibrium criterion  $C_{equ}$  remains as low as possible. It will be noted that the waypoints are here defined in the space of velocities instead of the geographic space as in §3.4 for performing a flight plan in automatic mode.

At each point of the reference trajectory between the selected waypoints the linear velocities are calculated. Taking account of the aircraft performance in longitudinal and vertical acceleration a first order filtering is used to calculate the velocities at every flight point joining the selected waypoints.

As an example, Figure 6 shows in the  $(U, V_z)$  plane a mapping of the equilibrium criteria when  $\lambda_2$  is jammed at a fixed value ( $\lambda_2=51\%$ , corresponding to the initial conditions of flight at  $U=40m/s$ ). In this plane, the dark blue lines correspond to the lowest values of the criterion.

In this example, between the initial flight conditions (black circle) at  $U=40m/s$ ,  $V_z=0$ , and the run-on landing conditions (red circle at  $U \sim 20m/s$ ,  $-2 < V_z < -1m/s$ ) a way in the  $(U, V_z)$  plane appears to be the most appropriated to follow. The value of the equilibrium criterion is indeed very low on this way.

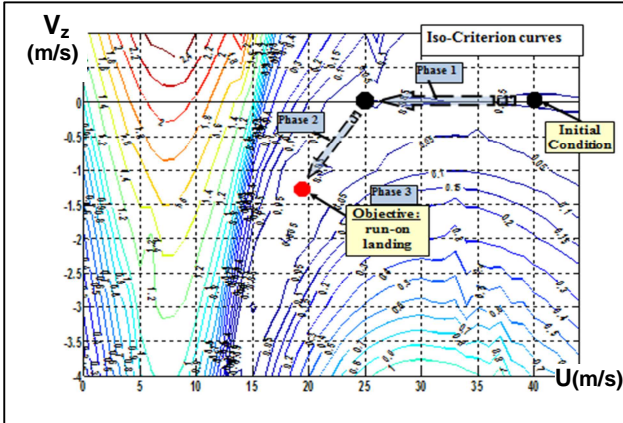


Figure 6: Definition in the  $(U, V_z)$  plane of the emergency procedure –  $\lambda_2$  jammed at 40m/s

To build the reference trajectory an intermediate waypoint can also be selected at  $U=25\text{m/s}$  and  $V_z=0$ .

### 5.3 Methodology to manage actuator failures

The methodology proposed to manage flight after detection of an actuator failure, then to perform a landing in emergency consists to:

- Select and plot the  $C_{equ}$  mappings corresponding to the value of the jammed actuator,
- Select the most appropriate waypoints (small  $C_{equ}$  value) to operate deceleration, descent, and landing,
- Calculate the reference trajectory joining the selected waypoints with account of aircraft performance and limits. The reference trajectory is then constituted of a series of successive flight phases delimited by the set of selected waypoints.
- Define for each waypoint the control objectives (the flight parameters to reach in priority),
- Determine for each waypoint, the prediction horizon the most adapted to a controlled and stabilised flight,
- Perform the emergency procedure in following the reference trajectory by means of the nonlinear model predictive control method. The transition from one flight phase to the next one is made as soon as the control objectives of the previous one are reached.

## 6. APPLICATIONS TO ACTUATOR JAMMING

### 6.1 Case 1 ( $\lambda_2$ Jamming at 40m/s, run-on landing)

In this first case, the actuator 2 jamming occurs at  $t=10\text{s}$  while aircraft is flying at level at 40m/s. Three seconds after the failure an emergency procedure is engaged. According to the methodology described in §5.3 the guidance strategy consists in three flight phases: a deceleration to  $U=25\text{m/s}$  at level, then a descent at  $V_z=-1\text{m/s}$  with a deceleration at 20m/s, and finally a run-on landing with account of ground effects (Figure 6). The parameters of the predictive control law have been defined as described earlier.

For two different weighting matrices: P1 (in black - all weights of parameters set equal to unit) and P2 (in red - only the velocity components and the route angle are set to 1) the Figure 7 shows versus the time horizon  $h=\rho.\Delta t$ :

- the highest real part of the eigen values of the state matrix  $F$  relative to the continuous form of the control equation (see Appendix 1) in (7.a),
  - the norm of the noise sensitivity matrix  $(TCE^P)$  in (7.b).
- These data allow guiding the choices in the control parameters. It can be noted that a time horizon value chosen between 2 and 3 seconds provides fairly good stability characteristics, and correlatively the weighting matrix P2 provides a control law that is less sensitive to state noises.

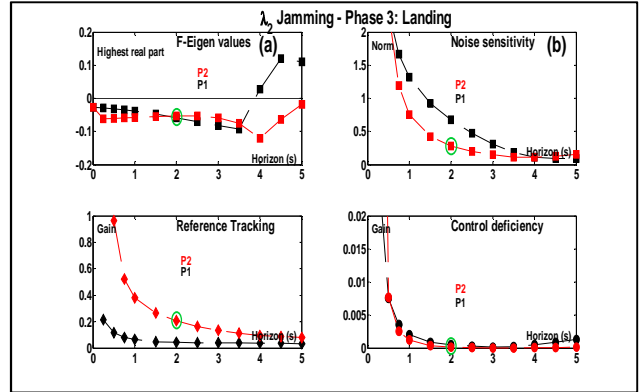


Figure 7 Effect of control parameters on system stability (7.a) and sensitivity to state noises (7.b)

To illustrate the effect of the control law, the comparison between the positions in the complex plane of eigen values for the system in open loop (o) and in closed loop (+) with  $h=2\text{s}$  is given in Figure 8 in the case of the landing phase. With the predictive control law the displacement towards the left side of the complex plane can be noted for some poles situated in open loop close to the instability area.

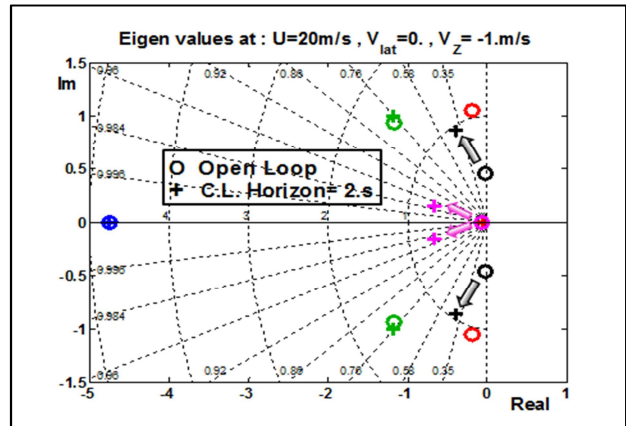
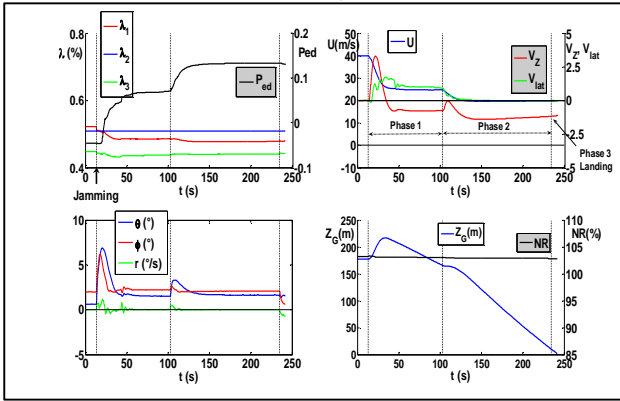


Figure 8: Eigen values in the complex plane for the system in open loop (o) and in closed loop (+)

The simulation results are presented in Figure 9. In these plots, the beginning of every flight phase is indicated by a vertical dashed line. The jamming of actuator occurs at  $t=10\text{s}$ . Three seconds later the automatic system takes over the aircraft flight control according to the methodology as defined previously. The control and stability of the flight are preserved in all phases up to the touch-down point. The landing phase is engaged as soon as aircraft height is less than 10m. At touch-down the simulation is stopped because the model is not representative of the rolling phase. Conditions

obtained at touch-down are very satisfactory:  $U \sim 20\text{m/s}$ ,  $V_{lat} \sim 0\text{m/s}$ ,  $V_z = -1.6\text{m/s}$ ,  $\theta = 1^\circ 5$ ,  $\phi = 0^\circ 6$ ,  $r = -0.8^\circ/\text{s}$ .



**Figure 9: Reconfiguration and run-on landing after  $\lambda_2$  actuator jamming**

In Figure 9 the actuator jamming occurs while aircraft is initially in stabilized flight. Now we consider the situation where the actuator jamming happens while the pilot is acting on the sticks and the aircraft engages a dynamic phase. Other conditions of the previous  $\lambda_2$  jamming scenario are kept similar. As shown in Figure 10 the pilot starts acting on the sticks at  $t=3\text{s}$ , then the  $\lambda_2$  jamming occurs at  $t=4.5\text{s}$  while flight parameters are dynamically evolving.

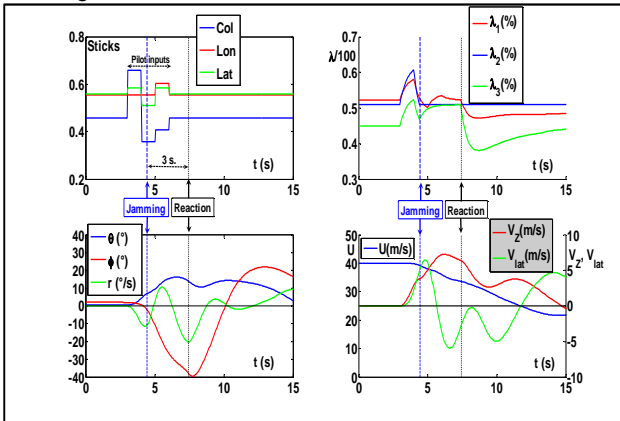


**Figure 10: Actuator jamming in a dynamic phase**

Simulation results are still satisfactory, the same type of landing is realised (Figure 11). Conditions at touchdown are:  $U \sim 19.4\text{m/s}$ ,  $V_{lat} \sim -0.4\text{m/s}$ ,  $V_z = -1.2\text{m/s}$ ,  $\theta = 2^\circ 2$ ,  $\phi = 2^\circ 0$ ,  $r = -1.9^\circ/\text{s}$ .

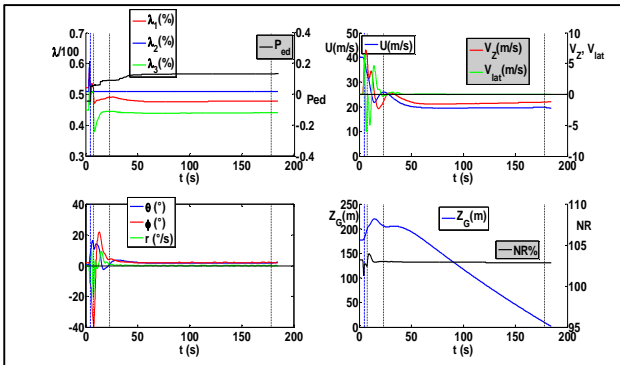


**Figure 11: Reconfiguration and run-on landing after  $\lambda_2$  actuator jamming while aircraft is in a dynamic phase**

Another issue of concern is the robustness of the method. In order to assess it, the simulation of the  $\lambda_2$  jamming scenario in Figure 9 (jamming at  $t=10\text{s}$ ) has been conducted with the inclusions of:

- random white noises on all state components,
  - North wind gusts ( $W_N$  in magenta) of  $5\text{m/s}$  for  $35 < t < 45\text{s}$  and of  $-5\text{m/s}$  for  $110 < t < 120\text{s}$ ,
  - East wind gust ( $W_E$  in cyan) of  $5\text{m/s}$  for  $170 < t < 180\text{s}$ ,
  - and a 10% shift of the aerodynamic coefficients in the prediction model with respect to the simulation model.
- Results presented in Figure 12 show a good robustness of the control method to these different disturbances. Conditions at touch-down are still satisfactory:  $U \sim 19.6\text{m/s}$ ,  $V_{lat} \sim 0\text{m/s}$ ,  $V_z = -1.2\text{m/s}$ ,  $\theta = 1^\circ 5$ ,  $\phi = 0^\circ 6$ ,  $r = -1.0^\circ/\text{s}$ .

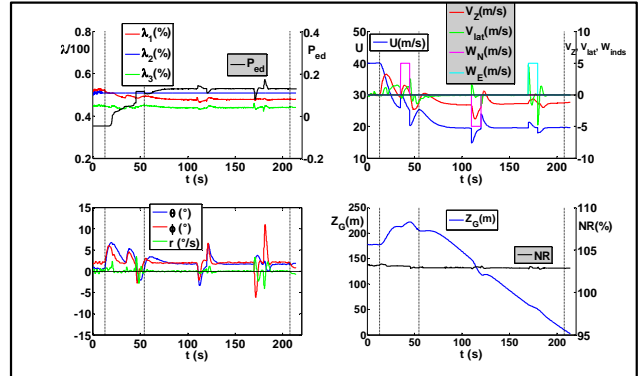


**Figure 12:  $\lambda_2$  actuator jamming scenario with the addition of state noises, wind gusts, and a shift of 10% on the predictive model**

To illustrate measurement state noises, in Figure 13 the 'actual' parameters (in blue), which are used to simulate the flight, are compared to the measured parameters (in red) used to calculate the control inputs.

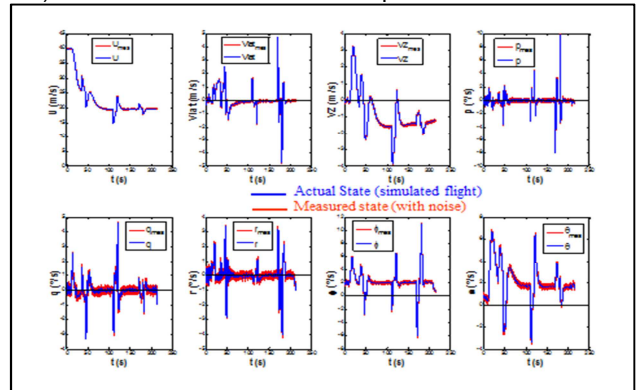


**Figure 13: Actual flight parameters (blue) compared to measured parameters (red) used to control aircraft**

## 6.2 Case 2 ( $\lambda_1$ Jamming at $40\text{m/s}$ , normal landing)

In the design of the swashplate the actuators  $\lambda_1$  and  $\lambda_2$  have different kinematic roles. Their influences for controlling the blade pitch angles are consequently different (see equation A2.3). So, it seems also interesting to test the case of a  $\lambda_1$  jamming with the proposed methodology. In the assessment simulations the same conditions as previously for  $\lambda_2$  jamming (Figure 11) are considered. In these conditions the kinematics effects of the  $\lambda_1$  jamming on the blade pitch angles accessibility are shown in Figure 14.



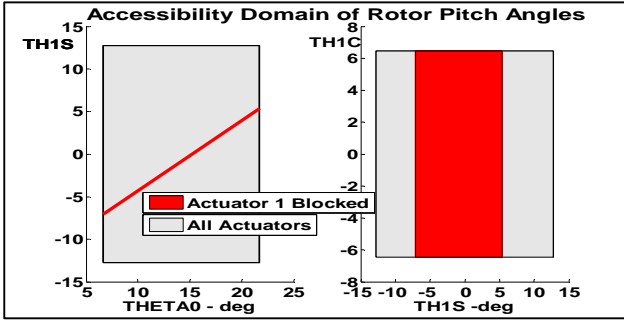


Figure 14: Effects of  $\lambda_2$  jamming on the pitch angles accessibility

In addition to a linear dependence between  $\theta_0$  and  $\theta_{1c}$ , it can be noted here a larger reduction in the range of the possible  $\theta_{1s}$  excursions (in red in Figure 14).

Considering this  $\lambda_1$  jamming case, the iso-criterion lines are plotted in the  $(U, V_z)$  plane as shown in Figure 15.

In this example, assuming the absence of any accessible runway a normal landing at low longitudinal speed is here required. To define the emergency procedure 4 waypoints (red points) are then chosen in this plane to keep aircraft as close as possible to flight conditions where the equilibrium criterion is low (Figure 15).

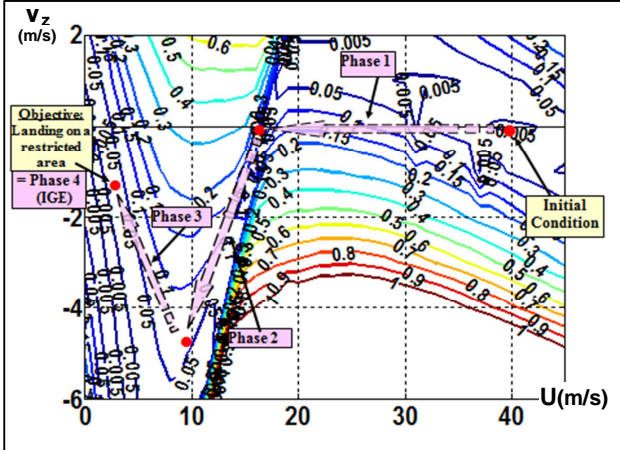


Figure 15: Definition in the  $(U, V_z)$  plane of the emergency procedure with  $\lambda_1$  jammed

The reference trajectory is then calculated as described previously. For the different flight phases, the time horizon of the predictive control law is chosen to ensure aircraft stability and, to a lower extent, to limit as much as possible the sensitivity of the trajectory to state noises and disturbances. For every flight phase, control objectives (values of flight parameters to reach) are then defined.

Figure 16 shows for two different flight phases: the descent (phase 2) and the landing (phase 4) the influence of the time horizon on the stability of the predictive control law. The comparison is also shown for two types of weightings: matrix P1 with weights set to 1 for all flight parameters and the weighting matrix P2, designed for landing objectives with only weights for  $V_z$ ,  $V_{lat}$ ,  $\theta$ ,  $\phi$  and  $r$ .

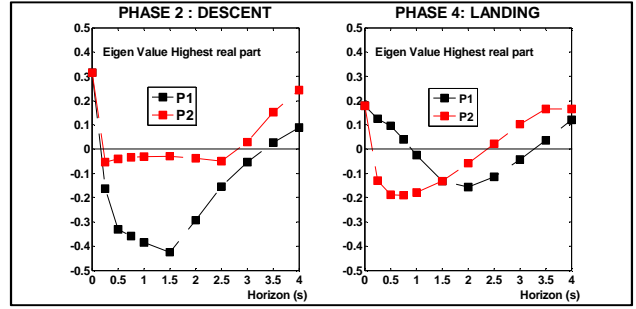


Figure 16: Effect of time horizon on stability in two flight phases: Descent (left) and Landing (right)

The control parameters have been chosen as follows: In phase 2 (descent):  $h=1.5s$  and P1 matrix, In phase 4 (landing):  $h=0.5s$  and P2 matrix.

Simulation results of this emergency landing are illustrated in figure 17. Measurement noises, wind gusts and a discrepancy of 10% in the aerodynamic coefficients between the simulation model and the prediction model are still present as in scenario of Figure 12.

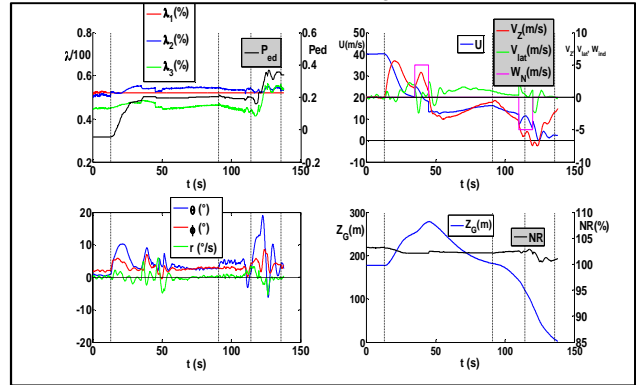
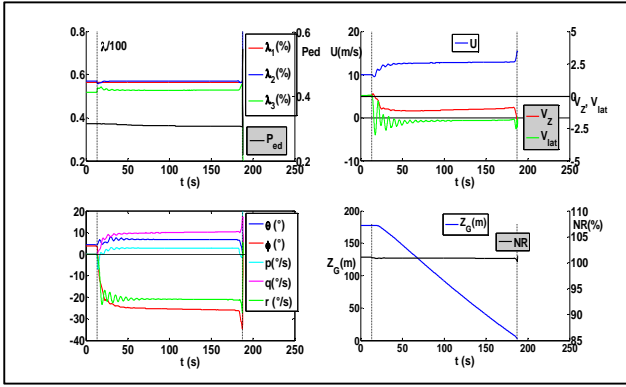


Figure 17: Emergency landing on a restricted area after  $\lambda_1$  actuator jamming

The landing phase is engaged as soon as aircraft height is less than 7m. At touchdown the aircraft parameters are:  $U=2.3m/s$ ,  $V_{lat}=-0.2m/s$ ,  $V_z=-1.9m/s$ ,  $\theta=2^\circ$ ,  $\phi=3^\circ$ , and  $r=0.3^\circ/s$ . The emergency procedure and the conditions of landing at low speed are again satisfactory.

### 6.3 Case 3 ( $\lambda_1$ Jamming at 10m/s, run-on landing)

In the previous scenarios, the actuator jamming was happening at initial flight conditions with a longitudinal speed of 40m/s. To extend the field of assessment a lower initial speed is now considered. Figure 18 presents the results of the methodology applied to a  $\lambda_1$  jamming scenario which occurs while aircraft is flying at a longitudinal speed of 10m/s.



**Figure 18: Reconfiguration and emergency landing after  $\lambda_1$  actuator jamming at  $U=10\text{m/s}$**

After actuator jamming, although the flight phase 1 was initially planned to fly at  $U=10\text{m/s}$  with a vertical speed  $V_z=-1\text{m/s}$ , the aircraft has been entering in a descent with a turn rate of about  $23^\circ/\text{s}$  with  $p\sim 3^\circ/\text{s}$ ,  $q\sim 10^\circ/\text{s}$ ,  $r\sim 21^\circ/\text{s}$ . The 3D trajectory in the earth axis system of the helicopter is illustrated in Figure 19.

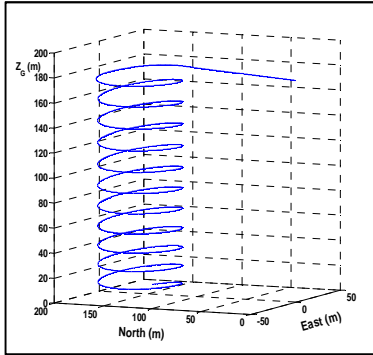


**Figure 19: 3D trajectory of aircraft after  $\lambda_1$  actuator jamming at  $U=10\text{m/s}$**

The descent is achieved at a vertical speed  $V_z = -0.9\text{m/s}$ , with a longitudinal speed  $U\sim 13\text{m/s}$  and a load factor  $N_z=1.13\text{g}$ .

This first flight phase after actuator jamming corresponds to a very stable equilibrium which acts as an attractor account of the actuator deficiency.

In Figure 20 are plotted for some equilibrium conditions the radius (20.a), the longitudinal speed (20.b), the engine torque (20.c) and the load factor (20.d) against the turn rate. This flight case (in red) corresponds to a turn radius of about  $33\text{m}$ .

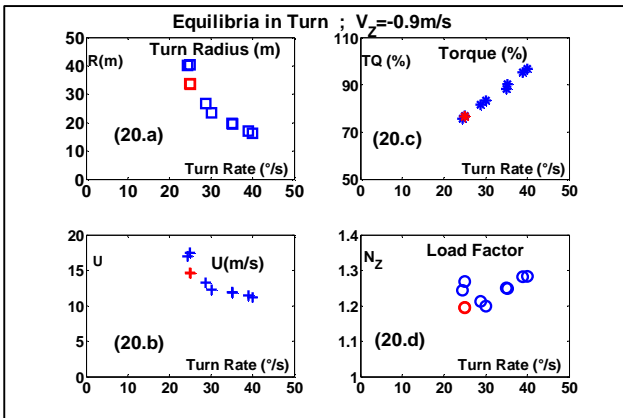


**Figure 20: Equilibria in turn rate at  $V_z=-0.9\text{m/s}$**

The last phase for landing is engaged when the aircraft height is at  $4\text{m}$  from the ground. This phase is a dynamic phase which conducts to the following landing conditions:

$U=15.2\text{m/s}$ ,  $V_{\text{lat}}=-1.6\text{m/s}$ ,  $\theta=8^\circ$ ,  $\phi=9^\circ$ ,  $r=-1^\circ/\text{s}$ ,  $q=2.2^\circ/\text{s}$  and  $p=91^\circ/\text{s}$ .

The conditions at landing are not optimal; to stop the turn rate before touchdown quick variations of actuators are necessary. A large roll rate still exists at touchdown however a fairly smoother landing could surely be obtained by optimising the height at which this last dynamic phase is engaged. Optimising the decision height for landing has not been investigated in the framework of this study.

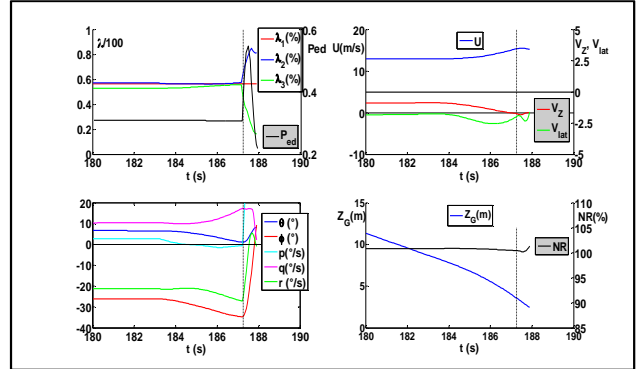


**Figure 21: Final phase of the emergency landing after  $\lambda_1$  actuator jamming at  $U=10\text{m/s}$**

## 7. CONCLUSIONS

The objectives of this study were studying and assessing the capabilities of a proposed trajectory following methodology. This methodology comprises a nonlinear predictive control law and a guidance strategy based on the definition of a series of waypoints. In case of actuator failure these waypoints are selected in the space of velocities with respect to the value of their equilibrium criteria.

The methodology includes a theoretical approach based on a local linearization of the flight system to guide the definition of the predictive control law parameters.

The methodology could proceed online and no assumption is required on the flight dynamics model which can be nonlinear and include various constraints on state and control variables.

Stability and robustness of the control law have been studied in different cases and scenarios with jamming of a swashplate actuator. Recovery and emergency procedures in such severe failures has been demonstrated to be feasible.

The methodology demonstrates fairly good performances in normal situation (automatic flight) as well as in case of a swashplate actuator jamming. In this latter situation the methodology permits to define an emergency procedure which tends to optimise the capabilities to keep control of flight and proceed to an emergency landing in conditions chosen as safe as possible.

Further developments could be still carried out. For instance the reference trajectory could be defined in following more accurately the way that minimises the equilibrium criteria at every point between two waypoints. As mentioned earlier another point of improvement would be to optimise the decision height of the landing phase. The calculations could also take account of the stochastic characteristics of the measurements to provide to the control law better estimates of the flight parameters. All

---

these developments could be integrated into this methodology to improve its performance. The use of realistic flight data would be also of actual benefit to carry out these developments.

The application of this methodology in helicopter avionics should consist of an automatic system which takes over the aircraft control as soon as a severe actuator failure is detected and proceeds to an emergency procedure with automation. Another option would be the use of a specific pilot assistance system but it seems difficult to develop and integrate on board such a system for this specific purpose.

Other applications of the methodology would be also possible, particularly in order to manage the flight in other failure cases like a tail rotor failure or a power loss of the control system.

The trajectory following method could also permit to estimate the necessary power and travels of actuators or control surfaces displacements to perform prescribed dynamic manoeuvres in various situations and in presence of disturbances. Such applications would be relevant to design and/or assess the control system of a new aircraft configuration. The results of this application could be also useful to specify data in the design process of the nominal control laws of the new aircraft configuration.

## 8. REFERENCES

[1] JTI-CS-2012-SGO-02-035 – Disconnect device for jam tolerant linear actuators  
[http://cordis.europa.eu/programme/rcn/17765\\_en.html](http://cordis.europa.eu/programme/rcn/17765_en.html)

[2] FASTDISC, FP7-JTI ongoing project  
[http://cordis.europa.eu/project/rcn/109749\\_en.html](http://cordis.europa.eu/project/rcn/109749_en.html)

[3] "Helicopter Flight-Control Reconfiguration for Main Rotor Actuator Failures", R. Enns, J. Si. *Journal of Guidance, Control, and Dynamics*, Vol.26, N°4, July-August 2003.

[4] « Model Predictive Heuristic Control: Applications to Industrial processes, J. Richalet, A. Rault, J.L. Testud, J. Papon. *Automatica*, 14, 413-428, 1978

[5] « Generalized Predictive Control", D. W. Clarke, C. Mohtadi, and P. S. Tuffs. *Automatica*, 1987

[6] « A survey of industrial model predictive control technology», S.J. Qin, T.A. Badgwell. *ELSEVIER Science*.  
<http://www.sciencedirect.com/science/article/pii/S0967066102001867>

[7] « Nonlinear Model Predictive Control », F. Allgöwer, R. Findeisen, C. Ebenbauer. *Control Systems, Robotics and Automation*, Vol XI

[8] « Model-Based Predictive Control – A Practical Approach», J.A Rossiter, *CRC PRESS*, 2005, London

[9] "Fault Detection and Reconfiguration applied to a Helicopter Swashplate Actuator", T. Rakotomamonjy, D. Trisranta, A. Cabut, 28<sup>th</sup> ICAS, 2012.

---

## Appendix 1: Control Equation in closed loop of the linearized system

Assuming that the nonlinear model can be locally linearized, the state and output equations of the model can be expressed as:  $\frac{d\hat{X}}{dt} = A \hat{X}(t) + B \delta(t)$  and  $\hat{Y}(t) = C \hat{X}(t)$

In the absence of any disturbance the discrete formulations of the model equations are:

- Model state equation:  $\hat{X}_{k+1} = E \hat{X}_k + \Delta t \cdot B \delta_k$  with  $E = I + \Delta t \cdot A$

- Model output vector equation:  $\hat{Y}_k = C \hat{X}_k$

The equation predicting the state at the next time step is:  $\hat{X}_{k+1|k} = E \hat{X}_k + \Delta t \cdot B \delta_k$

Assuming that the control input  $\delta_k$  is constant on the prediction horizon  $h=p \cdot \Delta t$ , we have:

$$\hat{X}_{k+2|k} = E \hat{X}_{k+1|k} + \Delta t \cdot B \delta_k = E^2 \hat{X}_k + \Delta t \cdot E B \delta_k + \Delta t \cdot B \delta_k$$

By recurrence it comes:  $\hat{X}_{k+p|k} = E^p \hat{X}_k + \Delta t \cdot \sum_{i=0}^{p-1} E^i B \delta_k$

That is:  $\hat{X}_{k+p|k} = E^p \hat{X}_k + H \delta_k$  with:  $H = \Delta t \cdot (E^p - I)(E - I)^{-1} B$

The predicted output vector is obtained from the following equation:

$$(A1.1) \quad \hat{Y}_{k+p|k} = C \hat{X}_{k+p|k} = C E^p \hat{X}_k + C H \delta_k$$

The control input is calculated to minimize:  $J_k = \frac{1}{2} (\hat{Y}_{k+p|k} - R_{k+p})^T P (\hat{Y}_{k+p|k} - R_{k+p})$

Substituting equation (A1.1) in  $J_k$  equation and deriving  $J_k$  with respect to  $\delta_k$  we get:

$$\frac{dJ_k}{d\delta_k} = H^T C^T P C H \delta_k + H^T C^T P (C E^p \hat{X}_k - R_{k+p})$$

At minimum we have: (A1-2)  $\frac{dJ_k}{d\delta_k} = 0$  so we can express the control input as a function of  $\hat{X}_k$  and  $R_{k+p}$

$$\delta_k = (H^T C^T P C H)^{-1} H^T C^T P (R_{k+p} - C E^p \hat{X}_k)$$

On the other hand, the linearized equations of the aircraft flight parameters are:

- System state equation:  $X_{k+1} = E (X_k + W_k) + \Delta t \cdot B \delta_k + v_k$  where:

$X_k$  is the actual state vector of the aircraft,

$W_k$  is a wind disturbance vector acting on the aircraft at  $t = k \cdot \Delta t$ . It will be noted that  $W_k$  is here expressed in the same reference axis system than the state vector.

$v_k$  is a Gaussian white vector of zero mean value.  $X_k = \hat{X}_k + v_k$  and  $Y_k = C X_k$

- System output equation:

$Y_k$  is the actual system output that is controlled in order to follow the reference vector  $R_k$ .

$\hat{X}_k$  is the state vector estimated with the model

$v_k$  is the noise existing on the state vector estimate. As shown hereafter, it is not needed to consider the measurement noise on the output vector components; only noise vector on state components is considered.

In the ideal case: no wind, no state noise, and full capability of controls, the control equation in closed loop is:

(A1-3)  $X_{k+1} = E X_k + \Delta t \cdot B \delta_k = S X_k + T R_{k+p}$  where:

$$S = (E - T C E^p) \quad T = \Delta t \cdot B (H^T C^T P C H)^{-1} H^T C^T P$$


---

To analyse stability of a dynamic system it sounds sometimes better to consider the system equations in their continuous expressions.

In the continuous form of the discrete control equation (A3-3), the state matrix  $F$  is related to the discrete state matrix  $E$  with the expression:

$$(A1-4) \quad F = \mathbf{E} - \mathbf{I} \gamma \Delta t$$

Now, we consider in the control equation three types of adverse terms for controlling the system: a control deficiency (e.g. low control effectiveness, actuator jammed or saturated, etc.), an existing wind disturbance  $\mathbf{W}_k$ , and an existing state noise vector  $\mathbf{v}_k$ .

- In case of control deficiency, by means of the control vector  $\delta_k$  (for  $\delta_k \in D$  the accessible domain of control), the equation A1-2 cannot be satisfied. Then at the minimum value of  $\mathbf{J}_k(\delta_k)$  we have:  $\frac{d\mathbf{J}_k}{d\delta_k} \neq 0 = d\mathbf{J}_{\min}$ .

It gives the new control vector:  $\delta_k = (\mathbf{H}^t \mathbf{C}^t \mathbf{P} \mathbf{C} \mathbf{H})^{-1} \mathbf{H}^t \mathbf{C}^t \mathbf{P} (\mathbf{R}_{k+p} - \mathbf{C} \mathbf{E}^p \mathbf{X}_k) + d\mathbf{J}_{\min}$

and the control equation in closed loop becomes:  $\mathbf{X}_{k+1} = \mathbf{S} \mathbf{X}_k + \mathbf{T} \mathbf{R}_{k+p} + \Delta t \cdot \mathbf{B} (\mathbf{H}^t \mathbf{C}^t \mathbf{P} \mathbf{C} \mathbf{H})^{-1} d\mathbf{J}_{\min}$

- If a wind disturbance vector is acting on the aircraft at  $t = k \cdot \Delta t$ , then we have:

$$\mathbf{X}_{k+1} = \mathbf{E} (\mathbf{X}_k + \mathbf{W}_k) + \delta t \cdot \mathbf{B} \delta_k$$

The model predictions and calculation of the control vector are carried out in the same way as previously, so that the control equation becomes:  $\mathbf{X}_{k+1} = \mathbf{S} \mathbf{X}_k + \mathbf{T} \mathbf{R}_{k+p} + \mathbf{E} \mathbf{W}_k$

- If there is any measurement noise on the state vector estimate:  $\hat{\mathbf{X}}_k = \mathbf{X}_k + \mathbf{v}_k$  then the control input becomes:

$$\delta_k = (\mathbf{H}^t \mathbf{C}^t \mathbf{P} \mathbf{C} \mathbf{H})^{-1} \mathbf{H}^t \mathbf{C}^t \mathbf{P} (\mathbf{R}_{k+p} - \mathbf{C} \mathbf{E}^p (\mathbf{X}_k - \mathbf{v}_k))$$

and the control equation in close loop is:  $\mathbf{X}_{k+1} = \mathbf{S} \mathbf{X}_k + \mathbf{T} \mathbf{R}_{k+p} + \mathbf{T} \mathbf{C} \mathbf{E}^p \mathbf{v}_k$

- Finally, taking into account these three types of undesired terms in the general expression of the closed loop control equation, we have:

$$\mathbf{X}_{k+1} = \mathbf{S} \mathbf{X}_k + \mathbf{T} \mathbf{R}_{k+p} + \mathbf{E} \mathbf{W}_k + \mathbf{T} \mathbf{C} \mathbf{E}^p \mathbf{v}_k + \Delta t \cdot \mathbf{B} (\mathbf{H}^t \mathbf{C}^t \mathbf{P} \mathbf{C} \mathbf{H})^{-1} d\mathbf{J}_{\min}$$

In this control equation it can be noted that:

- ✓ The main control parameter is  $p$  which defines the horizon length ( $h = p \cdot \Delta t$ ) of the time prediction. Another set of control parameters is the diagonal terms of the  $\mathbf{P}$ -matrix. These weighting terms allow giving more or less importance to some chosen flight parameters of the reference trajectory to follow.
- ✓  $\mathbf{S}$  is the state matrix of the discrete system. The stability will depend on the position of the  $S$ -eigen values in the complex plan with respect to the unit circle. Similarly, considering the state matrix ( $F$ ) of the system in its continuous form (A1-4), the stability will be obtained if all the real parts of its eigen values are negative.
- ✓  $\mathbf{T}$  is the transfer matrix between the reference target and the state vector. Globally it can be considered that the larger the norm of this matrix is, the larger is the gain to reach the target. If this gain is large, controls can be saturated to track reference.
- ✓  $\mathbf{E}$  is the sensitivity matrix of the state vector with respect to the disturbance vector (wind).
- ✓  $\mathbf{T} \mathbf{C} \mathbf{E}^p$  is the sensitivity matrix of the state vector with respect to its measurement noise vector. The larger the norm of this matrix will be, the more the state noise will perturb the control law.
- ✓  $\Delta t \cdot \mathbf{B} (\mathbf{H}^t \mathbf{C}^t \mathbf{P} \mathbf{C} \mathbf{H})^{-1}$  is the sensitivity matrix of the state vector with respect to control deficiencies.

---

## Appendix 2: Kinematic Relations of the Swashplate

A kinematics model of the swashplate has been developed<sup>[9]</sup> in order to simulate realistic failures of its actuators. A simplified but representative model has also been derived from its exact formulation and integrated into the flight mechanics simulation code of a generic helicopter. The swashplate mechanism is designed to control the blade pitch angles ( $\theta_i$ ) through the elevation and angular positions of the rotating plate. Blades are linked to the plate by means of rods. These 3 degrees of freedom of the swashplate are obtained through the extension of 3 vertical actuators ( $\lambda_i$ ).

So, three sets of parameters are distinguished here:

- the pilot commands on the sticks ( $C_{OL}$ ,  $L_{ON}$ ,  $L_{AT}$ ),
- the swash plate actuator elongations ( $\lambda_1$ ,  $\lambda_2$ ,  $\lambda_3$ ),
- and the blade pitch angles ( $\theta_0$ ,  $\theta_{1s}$ ,  $\theta_{1c}$ ).

The kinematic equations expressing relations between actuator elongations and pitch angles are as follows:

$$\begin{aligned} \lambda_1 &= e\theta_0 - \sigma R\theta_{1s} \\ (A2.1) \quad \lambda_2 &= e\theta_0 + \sigma R\theta_{1c} \\ \lambda_3 &= e\theta_0 - \sigma R\theta_{1c} \end{aligned}$$

$$(A2.2) \quad 1/\sigma^2 = 1 - \theta_{1s}^2 - \theta_{1c}^2$$

where R is the plate radius and e is the blade rod eccentricity.

Inversely the relations providing pitch angles as function of the actuators are:

$$(A2.3) \quad \begin{aligned} \theta_0 &= \frac{1}{2e} (\lambda_2 + \lambda_3) \\ \theta_{1s} &= \frac{1}{\sigma R} \left( \frac{\lambda_2 + \lambda_3}{2} - \lambda_1 \right) \\ \theta_{1c} &= \frac{\lambda_2 - \lambda_3}{2\sigma R} \end{aligned}$$

$\sigma$  can also be expressed as a function of the actuator elongations:

$$(A2.4) \quad \sigma^2 = 1 + \left( \frac{\lambda_2 - \lambda_3}{2R} \right)^2 + \frac{1}{R^2} \left( \lambda_1 - \frac{\lambda_2 + \lambda_3}{2} \right)^2$$

If the actuator  $\lambda_1$  is jammed to a constant value,  $a$  for instance, then we have:  $a = e\theta_0 - \sigma R\theta_{1s}$ . This is a dependence relationship between  $\theta_0$  and  $\theta_{1s}$  that is quasi linear. Indeed, as long as  $\theta_{1c}$  and  $\theta_{1s}$  are fairly small with respect to 1, then in the equation (A2.2) the terms  $\theta_0^2$  and  $\theta_{1s}^2$  are very small with respect to 1 so that  $\sigma \sim 1$ . The dependence relationship between  $\theta_0$  and  $\theta_{1s}$  is consequently very close to a linear one. Similarly, the jamming of the actuator  $\lambda_2$  to a constant value leads to a quasi linear relationship between  $\theta_0$  and  $\theta_{1c}$ .

---